29th Congress of the International Council of the Aeronautical Sciences
St. Petersburg, Russia; September 7-12, 2014

FLEXIBLE FORMATION SHAPE CONTROL BASED ON THE LOCAL INTERACTION AMONG AIR VEHICLES

Yoshinobu Inada
Course of Aerospace, Department of Aeronautics and Astronautics, School of Engineering, Tokai University, Japan

Keywords: *Formation Shape Control, Air vehicle, Local Interaction*

Abstract

The local interaction based flexible formation shape control was investigated which realized a formation shape change utilizing the similarity of formation shape and the shape of interaction field. The control was realized by a simple method of adjusting the shape of interaction field around each vehicle. The number of DOF to be controlled was then reduced into a few shape parameters of the interaction field, thus effectively preventing the divergence of DOF in the formation shape control.

1 Introduction

Aerial information gathering or reconnaissance by using multiple air vehicles is a feasible method to cover a wide search area and realize simultaneous observation at different points. This kind of survey system is generally called "sensor network[1,2]". Although its availability and convenience, the control of flight formation with multiple air vehicles has technical difficulties because the degree of freedom to control the whole system increases as the number of vehicles involved in the formation increases, e.g. the position and the velocity of all vehicles must be controlled correctly to avoid collisions among vehicles and to navigate them in security to the destination. Thus, the control load inevitably increases as the number of vehicles increases.

In this study, as an approach to prevent the divergence of control load, the local interaction based flight formation control was investigated. In the local interaction based control, the motion of each vehicle is controlled autonomously, i.e. the velocity and the moving direction of each vehicle is determined locally based on the interaction of the vehicle with its neighbors, thus eliminating the concentration of control load on a single commander.

When a formation takes a certain shape, each vehicle's position need to be adjusted. A good example is an acrobat flight formation in an air show. Each vehicle in a formation takes the adequate position to form a certain shape, e.g. straight line, V-shape formation, etc. In this conventional flight formation control, the control load tends to concentrate on the commander because it always needs to know the situation of all followers and give commands to them. Then this is not applicable to the large scale formation composed of tens or hundreds of vehicles.

The local interaction based formation control plays an important role in a reduction of control load in the formation shape control. This control utilizes the similarity of formation shape and the shape of interaction field[3], eliminating the complicated process of position calculation. The details is explained in the following sections.

2 Method

2.1 Flight Formation Control

The local interaction based control in this study uses three interactions among air vehicles, i.e. "attraction", "repulsion", and "parallel orientation", to realize the formation[4,5]. "Attraction" makes the vehicle approach to its neighbors; "repulsion" makes the vehicle move

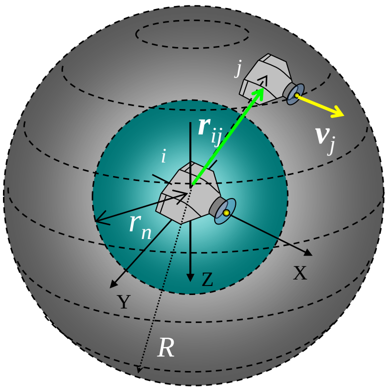

Fig. 1 Interaction Field

away from its neighbors to avoid collision. These two interactions are used to secure the inter-vehicle distance and then switched from one to another according to the distance between vehicles so that the repulsion operates when the distance between vehicles is small and the attraction operates when the distance is large, while the parallel orientation always operates to navigate all the vehicles in the same direction. These interaction rules can simply be formulated as follows by referring to the interaction field set around the vehicle as shown in Fig. 1:

$$\boldsymbol{A}_{ij} = A\left(|\boldsymbol{r}_{ij}| - r_n\right)\frac{\boldsymbol{r}_{ij}}{|\boldsymbol{r}_{ij}|} \tag{1}$$

$$\boldsymbol{P}_{ij} = P\frac{\boldsymbol{v}_j}{|\boldsymbol{v}_j|} \tag{2}$$

$$\boldsymbol{\alpha}_{ij} = \boldsymbol{A}_{ij} + \boldsymbol{P}_{ij} \tag{3}$$

where $\boldsymbol{A}_{ij}$ is the attraction-repulsion vector and $\boldsymbol{P}_{ij}$ is the parallel orientation vector; A and P are the attraction-repulsion gain and the parallel orientation gain, respectively; $\boldsymbol{r}_{ij}$ is the position vector of the *j-th* vehicle with respect to the *i-th* vehicle, and $|\boldsymbol{r}_{ij}|$ is the distance between the *i-th* and the *j-th* vehicle; r_n is the neutral distance where the attraction and repulsion balance; $\boldsymbol{v}_j$ is the velocity vector of the *j-th* vehicle; $\boldsymbol{\alpha}_{ij}$ is the interaction vector between the *i-th* and the *j-th* vehicles, R is the radius of the interaction field. When the *i-th* vehicle interacts with multiple neighbors in the interaction field, $\boldsymbol{\alpha}_{ij}$ is

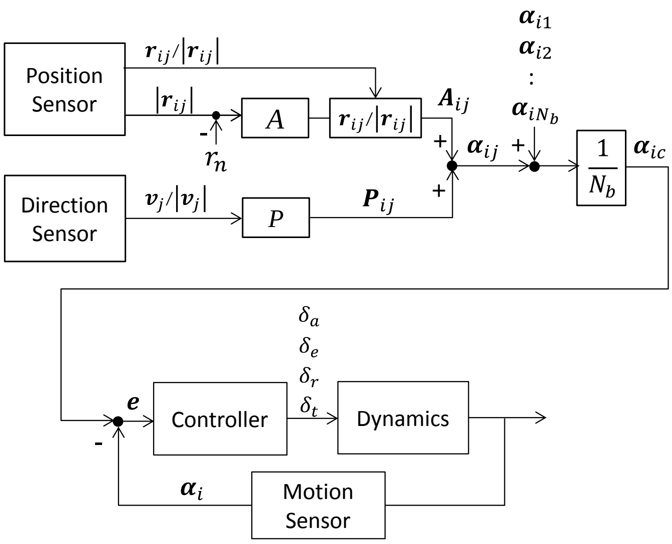

Fig. 2 Block diagram of flight formation control

averaged by using the following equation and the command vector of the *i-th* vehicle $\boldsymbol{\alpha}_{ic}$ is calculated.

$$\boldsymbol{\alpha}_{ic} = \frac{1}{N_b}\sum_{j=1}^{N_b}\boldsymbol{\alpha}_{ij} \tag{4}$$

where N_b is the number of neighbors in the interaction field and usually has the upper limit $N_{b,max}$ $\left(N_b \le N_{b,max}\right)$ to consider the limit of sensing ability. The *i-th* vehicle is controlled to advance in the direction of vector $\boldsymbol{\alpha}_{ic}$ at the speed proportional to the length of vector $\boldsymbol{\alpha}_{ic}$. The block diagram of this control is shown in Fig. 2, where $\delta_a, \delta_e, \delta_r$ are the angle of aileron, elevator, and rudder, and δ_t is the throttle value calculated by the controller (PID controller); $\boldsymbol{\alpha}_i$ is the motion vector which orients in the current moving direction of the *i-th* vehicle and its length is proportional to the current speed of the *i-th* vehicle.

2.2 Formation Shape Control

The formation shape control in this study is based on the geometrical similarity between the shape of interaction field and the formation shape[3]. The basic mechanism is shown in Fig, 3. Neighbors existing in the interaction field of a

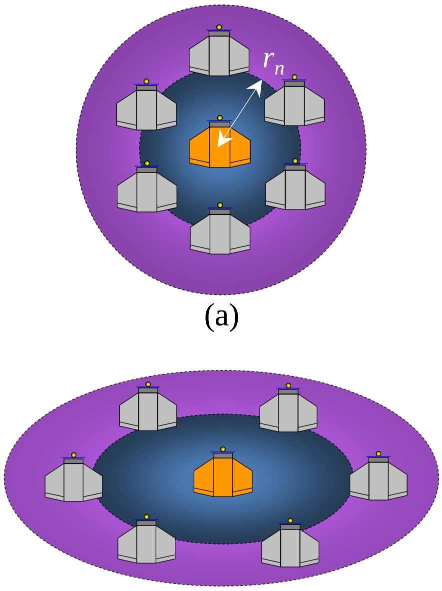

(a)

(b)

Fig. 3. Shape of interaction field and position of neighbors

certain vehicle tend to exist around the surface of sphere with the radius r_n because the attraction and the repulsion balance on this surface (hereafter this surface is called "neutral surface"). When the shape of interaction field is sphere, the neighbors takes approximately the same distance r_n from the vehicle, forming a spherical distribution around the vehicle as shown in Fig. 3(a). This situation also happens in all other vehicles in the formation, resulting in a sphere shape of formation. When the shape of interaction field is modified into another shape, e.g. an ellipse, then the neighbors will take the elliptical distribution around the vehicle as shown in Fig. 3(b). The final shape of formation in this case will, then, become like an ellipse. Consequently, a simple and low load formation shape control is realized by using the similarity of the shape of the interaction field and the formation shape.

However, this method has a problem. The distance between vehicles is sensed by the distance sensor like an ultrasonic sensor. If the vehicle needs to change the sensitivity of distance sensor depending on the direction, e.g. short range sensitivity in the short axis and long range sensitivity in the long axis of ellipse as shown in Fig. 3(b), the vehicle has to carry sensors with different sensitivity. Those sensors usually need power sources with different voltages. So, this method is not practical for small vehicles which have small payload and limited power sources.

Here, the virtual transformation method is proposed. Scaling vector $\boldsymbol{D} = \left(k_x, k_y, k_z\right)$ is introduced where k_x, k_y, k_z are the scaling parameters in the x, y, z direction of the vehicle fixed coordinate system, respectively. When the vehicle has a neighbor and its position vector is $\boldsymbol{r}_{ij} = (x_{i,j}, y_{i,j}, z_{i,j})$, each component of the vector is multiplied by the corresponding scaling parameter as follows:

$$\boldsymbol{D}_{ij} = \left(k_x x_{i,j}, k_y y_{i,j}, k_z z_{i,j}\right) \qquad (5)$$

When $\left|\boldsymbol{D}_{ij}\right|$ is used as the distance between vehicles in equation (1) like

$$\boldsymbol{A}_{ij} = A\left(\left|\boldsymbol{D}_{ij}\right| - r_n\right)\left(\boldsymbol{r}_{ij}/\left|\boldsymbol{r}_{ij}\right|\right), \quad (6)$$

the interaction field around the vehicle can be virtually expanded by $1/k_x, 1/k_y, 1/k_z$ times in each x, y, z direction, respectively. The neighbors then tend to be allocated around this modified interaction field surface, thus resulting in the expansion of formation shape in each direction.

The motion of each vehicle is calculated by using the six degrees of freedom Newtonian equation of motion. The parameters of each vehicle used in the calculation are shown in Table 1, which are from the real micro air vehicle in the literature[6)].

The expansion of formation is used to evaluate the formation shape, which is the average of the absolute value of coordinate of vehicle on each axis of the formation fixed coordinate system. The origin of coordinate system is taken at the average position of all vehicles and the x-axis is taken in the moving direction of the formation. The expansion along each axis is given as follows:

$$E_x = \frac{1}{N}\sum_{i}^{N}\left|x_{f,i}\right|, \quad E_y = \frac{1}{N}\sum_{i}^{N}\left|y_{f,i}\right|,$$

$$E_z = \frac{1}{N}\sum_{i}^{N}\left|z_{f,i}\right| \qquad (7)$$

where N is the number of vehicles in the formation and $x_{f,i}$, $y_{f,i}$, $z_{f,i}$ are the x, y, z coordinate of the i-th vehicles on the formation fixed coordinate system, respectively.

Table 1 Parameter of air vehicle

Main wing		
Area	S (m^2)	0.135
Span length	b (m)	0.6
Mean aerodynamic chord length (mac)	$\bar{c}$ (m)	0.2
Position of aerodynamic center	h_{nw} (mac)	0.25
Aspect ratio	AR	2.667
Effective aspect ratio	AR_e	2.133
Taper Ratio	λ	1.0
Sweepback angle	Λ (deg)	5.0
Dihedral angle	Γ (deg)	5.0
Lift curve slope	a_w	3.243
Horizontal tail		
Area	S_h (m^2)	0.02
Span length	b_h (m)	0.2
Aspect ratio	AR_h	2.0
Effective aspect ratio	$AR_{e,h}$	1.6
Sweepback angle	Λ_h (deg)	5.0
Lift curve slope	a_h	2.793
Position of aerodynamic center	l_h (m)	0.55
Tail volume	V_h (m^3)	0.407
Vertical tail		
Area	S_v (m^2)	0.01
Span length	b_v (m)	0.1
Aspect ratio	AR_v	1.55
Effective aspect ratio	$AR_{e,v}$	1.24
Sweepback angle	Λ_v (deg)	5.0
Lift curve slope	a_v	2.405
Position of aerodynamic center (horizontal)	l_v (m)	0.55
Position of aerodynamic center (vertical)	z_v (m)	0.05
Tail volume	V_v (m^3)	0.068
Fuselage		
Volume	V_f (m^3)	0.0004
Length (Body Length)	L (m)	0.33
Moment of inertia		
	I_{xx} (m^{2}kg)	0.011
	I_{yy} (m^{2}kg)	0.013
	I_{zz} (m^{2}kg)	0.007
	I_{xz} (m^{2}kg)	0.0006
Position of center of gravity (C.G.)	h_{CG} (mac)	0.15
Weight	W (kgf)	0.27
Total drag coefficient	C_{D0}	0.1

3 Results and Discussion

When the scaling parameters were changed, the formation shape was changed. Figure 4 shows the example of formation shape change where k_y was originally 0.0 and changed to 4.0. The shape was originally round (Fig. 4(a)) and finally became a laterally expanded shape (Fig. 4(b)). Figure 5 shows the time variation of expansion. The scaling parameter k_y was gradually changed from 0.0 to 4.0 from 0 to 250 step (1 step = 0.1 sec). The expansion along y axis E_y gradually increased and became almost constant after 500 steps (=50sec) while expansions along other axes E_x, E_z remained almost unchanged from the initial step. Figure 6(a) shows the relationship between the scaling parameter k_y and the expansion along each axis. The expansion along y axis E_y linearly increased as k_y increased. Figure 6(b) shows the relationship between the scaling parameter k_z and the expansion along z axis E_z. The linearity was also confirmed between k_z and E_z. These results mean the similarity between the shape of interaction field and the formation shape

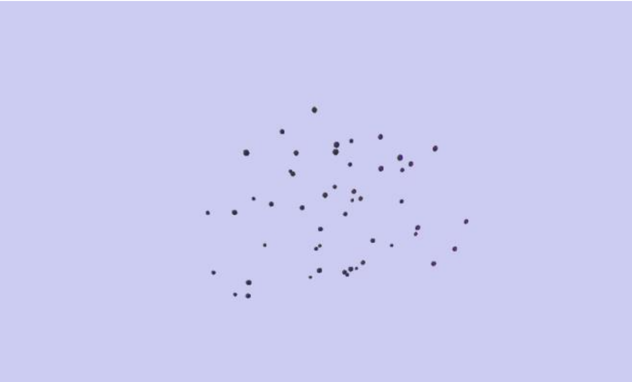

(a) Initial formation

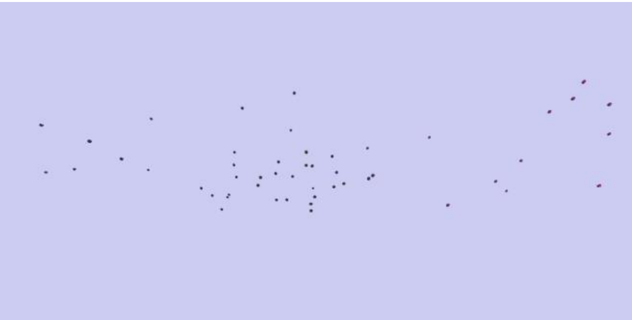

(b) Laterally expanded formation

Fig.4 Formation shape change

obviously exists. Thus the lateral and the vertical expansion of formation shape were successfully controlled by using the scaling parameters. In the conventional manner, the formation shape was controlled by assigning the position of each vehicle to fit a certain shape. When the shape is changed, the new position of all vehicles need to be calculated at every intermediate stage as well as at the final stage. This is a cumbersome process and thus the proposed method can provide a simple and feasible way to control the formation shape.

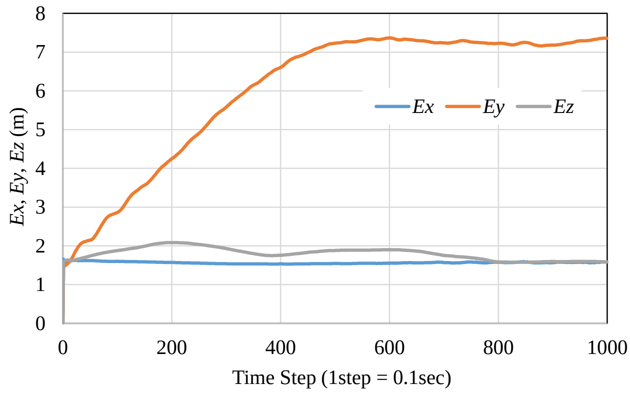

Fig. 5 Time variation of expansion

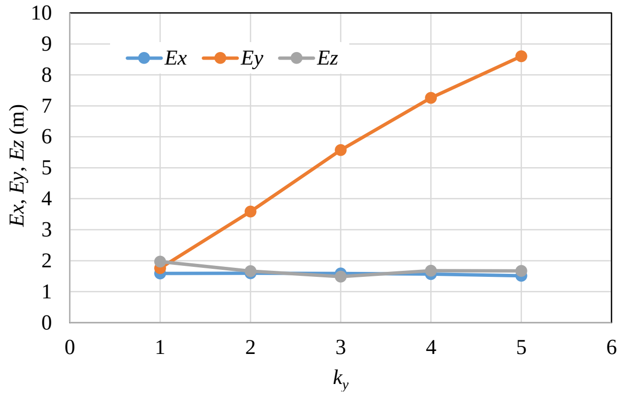

(a) k_y vs. E_x, E_y, E_z

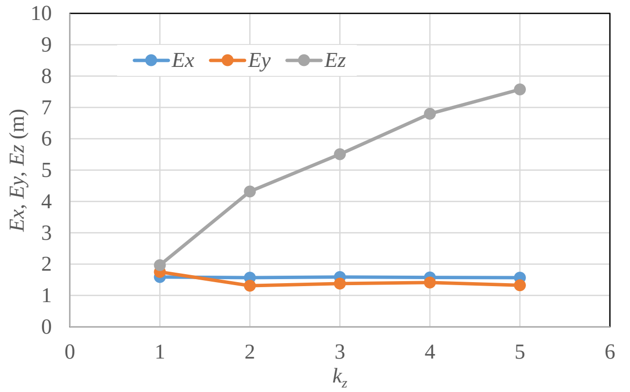

(b) k_z vs. E_x, E_y, E_z

Fig.6 Relationship between scaling parameter and expansion

References

[1] Yick, J., Mukherjee, B., and Ghosa, D.:Wireless sensor network survey, *Computer Networks*, **52** (12), pp. 2292–2330, 2008.

[2] Akyildiz, I. F., Su W., Sankarasubramaniam, Y., and Cayirci E.: A survey on sensor networks, *IEEE Communications Magazine*, **40** (8), pp. 104–112, 2002.

[3] Takahashi, R. and Inada, Y.: Formation Shape Control of Uumanned Air Vehicles, *Proceeding of the 28th International Congress of the Aeronautical Sciences (ICAS 2012)*, 2012.

[4] Inada, Y. and Takanobu, H.: Dependency of Collective Motion Control of Air Vehicles on Interaction Parameters, *Theoretical and Applied Mechanics Japan*, **58**, pp.185-195, 2010.

[5] Inada, Y. and Takanobu, H.: Flight-Formation Control of Air Vehicles Based on Collective Motion Control of Organisms, *Proceedings of the 18th IFAC Symposium on Automatic Control in Aerospace*, 2010.

[6] Fujinaga, J., Tokutake, H., and Sunada, S.: Flight Controller Design and Autonomous Flight Tests of 60cm-sized UAV, *7th European Micro Air Vehicle Conference and Flight Competition, Toulouse, France, September*, pp.17-21, 2007.

Copyright Statement